Desalination and Water Treatment
www.deswater.com
doi: 10.1080/19443994.2012.749246

51 (2013) 2656–2665
March

Taylor & Francis
Taylor & Francis Group

Cellulose triacetate forward osmosis membranes: preparation and characterization

Gang Li[a,b], Xue-Mei Li[a], Tao He[a,*], Biao Jiang[a], Congjie Gao[b]

[a]*Shanghai Advanced Research Institute, Chinese Academy of Sciences, 99#, Haike Road, Pudong New Area, Shanghai, China*
Tel. 00862120325162; Fax: 00862120325034; email: het@sari.ac.cn
[b]*College of Chemistry and Chemical Engineering, Ocean University of China, 238#, Songling Road, Laoshan District, Qingdao, Shandong 266003, China*

Received 2 March 2012; Accepted 30 August 2012

ABSTRACT

Cellulose triacetate (CTA) forward osmosis membranes were prepared by immersion precipitation. Following a standard recipe for the preparation of reverse osmosis membranes, the concentrations of polymer, additives (lactic acid, methanol), and solvent composition in the casting solution were investigated with respect to membrane permeation and salt rejection. The membrane preparation parameters including the evaporation time and the coagulation bath temperature were investigated as well. A CTA membrane with a quasi double-skinned morphology was obtained. The CTA FO membrane showed a water flux higher than 10 kg/m^2 h using 2 M glucose water solution as the draw solution and 0. 5 M NaCl as feed. A NaCl rejection of 95% was obtained.

Keywords: Forward osmosis; Membranes; Cellulose triacetate; Desalination

1. Introduction

Forward osmosis (FO), also known as osmosis, is a natural physical phenomenon [1–3]. In an FO process, water diffuses across a semipermeable membrane from a region of higher water chemical potential (lower osmotic pressure) to a region of lower water chemical potential (higher osmotic pressure) [4]. The FO process may require lower energy for pure water production and the system appears to be more fouling resistant than RO processes [5]. Moreover, FO shows a high water recovery rate up to 90% [6]. Potential applications of FO include seawater desalination, wastewater treatment [6–9], food and beverage [10,11], osmotic engine in drug release [12,13], and power generation [14]. There exist a number of technical barriers that impede FO's industrial applications. The major challenges are the lacks of ideal draw solution and high-performance membranes.

The development of membranes is of key importance for industrial application of FO. RO membranes have been tested and a considerably low water flux was frequently observed. A high-performance FO membrane is supposed to have the following characteristics [12]:

(1) hydrophilic dense active layer for high rejection rate and high water flux;
(2) thin porous support layer and high porosity;
(3) high mechanical strength; and

*Corresponding author.

(4) chemically resistant to acid and alkali solutions, and adaptable to wide pH value.

A commercial FO membrane has been developed by Hydration Technologies Inc. (HTI), which was believed to be made of cellulose triacetate (CTA) or a mixture of CTA and its derivatives. This membrane showed a higher water flux than commercial RO membrane. However, the water flux was much low than expected. For example, Elimelech et al. [15] reported about 80% lower than expected water permeability using HTI membrane and ammonia-carbon dioxide draw system.

The much lower than expected fluxes in the FO processes are generally ascribed to external and internal concentration polarizations (ICP), because of the water transfer causing concentration gradient between the bulk and near the membrane (external concentration polarization, ECP) and concentration gradient inside the membrane (ICP). The ECP can be reduced by optimization of the hydraulic status of the fluids. However, ICP is mainly controlled by the membrane porous support structure and membrane orientation [16]. During FO processes, the solute molecules diffusing inside the pores of the FO membrane are diluted or concentrated due to the water transfer, which causes a concentration difference between that inside of the pores and bulk solution. Depending on the membrane orientation, two operation modes are identified as active layer facing the draw solution (AL-DS mode) and active layer facing the feed solution (AL-FS mode). In general in AL-DS mode, less ICP is expected and thereby higher water fluxes are observed. In the AL-FS mode, because the draw solution is facing the porous support, solute reverse diffusion may become significant which further deteriorate the degree of ICP [17]. To quantify the degree of ICP, Gerstandt et al. [18] proposed a membrane structure parameter S, as

$$S = \frac{t\tau}{\varphi} \tag{1}$$

where t, τ, and φ represent the membrane thickness, tortuosity, and porosity, respectively. A low S value indicates a low degree of internal concentration polarization. Accordingly, a good FO membrane should have a low-membrane thickness, low tortuosity, and high porosity. Practically, it is difficult to realize since thinner membrane has a low mechanical strength and the control of membrane tortuosity and porosity is not straightforward.

So far, many approaches have been utilized for the FO membrane preparation including phase inversion [19], interfacial polymerization [20,21], and layer-by-layer deposition [22]. Although interfacial polymerization has shown good potentials for the preparation of RO type membrane, the membranes prepared as such are asymmetric, where severe ICP is unavoidable. It is believed membranes with double skins can help to reduce or avoid ICP and thus good FO performance is expected [23]. Although many research works reported the preparation and performance of the "double skin" FO membranes, the performance of this membranes are yet not satisfactory.

For example, Chung et al. [24] have reported the preparation of double-skinned cellulose acetate (CA) FO flat-sheet membranes. A prototype double-skinned CA FO membrane prepared by phase inversion showed a water flux of 48.2 L/m^2 h using 5.0 M $MgCl_2$ as the draw solution at 22˚C. However, this membrane showed about a 40% lower flux when the orientation of the membrane is changed from bottom mode to top mode. Moreover, a very high solute reverse diffusion was observed in comparison to many research works, which hampers its applicability. Recently, Su et al reported the hollow fiber type of the CA membrane [25]. In FO tests, the CA hollow fiber membrane with inner selective layer generates a water flux of 17.1 L/m^2 h with 2.0 M $MgCl_2$ draw solution and DI water feed (AL-DS mode). However, the same problems of very high solute reverse flux remains unsolved.

Overall, cellulose acetate appears to be a good candidate for FO membrane preparation with respect to permeability probably due to its good hydrophilicity. However, the high reverse solute flux hampers its application potentials. Improvement in the membrane structure to reduce the reverse solute flow may help the development of FO membranes with satisfactory FO performance.

In this report, we describe the development of FO membranes from CTA with two compact surfaces. A dioxane and acetone mixture was used as the solvent. Lactate and methanol were used as nonsolvents. The membrane preparation was optimized with respect to the polymer and additive concentrations and parameters for immersion precipitation. The FO performance of the membrane was tested using glucose as a draw agent and NaCl solution as the feed and compared with HTI membrane in desalination. The underneath reasons that cause performance difference was explored, which might help for the development FO membranes for large-scale applications.

2. Experimental

2.1. Materials

Cellulose triacetate (CTA) was purchased from Wuxi Institute of Chemical Engineering with an acyla-

tion degree of 43.3%. Cellulose acetate (CA) was obtained from Sinopharm Chemical Reagent Co., Ltd. with an acylation degree of 39.2%. Analytical grade sodium chloride, glucose, dioxane, acetone, lactic acid, and methanol are obtained from Sinopharm. Deionized water was used for permeability and rejection test. Commercial FO membranes were provided by Hydration Technologies Inc. (HTI).

2.2. Membrane preparation

Dried polymers (CTA or/and CA) were added to three-necked flask equipped with a mechanical stirrer containing a premixed solvent of dioxane, acetone, lactic acid, and methanol at a certain ratio. The solution was kept at 30°C and stirred till a homogeneous solution was obtained. The solution was then stored in an oven at 30°C for several hours to de-aerate. Membranes were prepared by casting the polymer solution onto a dry clean glass plate and immersed into a water bath within 3 s at 12°C if not otherwise stated. The casting knife was 200 μm. After solidification, the membranes were immersed in deionized water for 24 h before test.

2.3. FO performance test

A lab-scale forward osmosis setup is schematically shown in Fig. 1. The test cell consists of two rectangular plastic symmetric half cells with the membrane in between. The dimensions inside the half cell are 10 cm × 3 cm × 0.3 cm in length, width, and height, respectively. A 0.5 M NaCl aqueous solution about 1.5 kg was used as feed and a glucose solution about 1.7 kg of 2 M if not other stated was used as the draw solution. Both feed and draw solutions were circulated using gear pumps in a concurrent flow mode to reduce the strain on the suspended membrane. An optimal flow rate was set at 3 L/min to reduce the external concentration polarization. Both feed and draw solutions were maintained at the same temperature by two thermostatic baths. Electronic thermometers with accuracy of 0.1°C were used to detect the solution temperature at the inlet and outlet of the module.

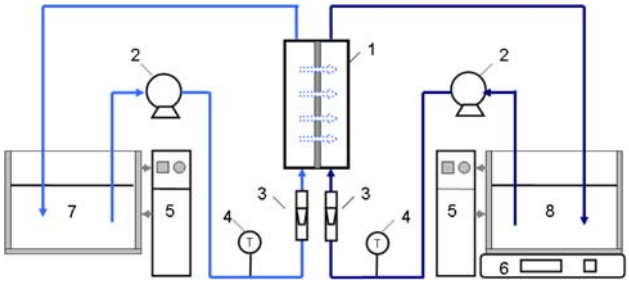

Fig. 1. Schematic illustration of the benchscale forward osmosis (FO) system. 1. FO test cell. 2. Gear pump. 3. Flow meter. 4. Thermometer. 5. Thermostat. 6. Weighting scale. 7. Feed tank. 8. Draw solution tank.

Water flux (J) was calculated as follows:

$$J = \frac{\Delta m}{S * \Delta t} \tag{2}$$

where Δm, S, and Δt are the weight (kg) of water passing through the membrane, the membrane area (m^2), and the time duration for collecting permeate (h), respectively.

Salt rejection rate of FO membrane was determined as follows:

$$R = \left(1 - \frac{C_p}{C_f}\right) * 100\% \tag{3}$$

where C_f and C_p are the NaCl concentrations in the feed solution and in permeate water via diffusion through the membranes (M). C_p was calculated by the amount of NaCl diffused into the draw solution divided by the water diffusing from the feed solution to the draw solution. In order to determine the salt passing through the FO membranes, the effect of the glucose concentration was considered.

The salt concentration was determined by measuring the conductivity of the glucose draw solution before and after experiment. Because the conductivity of salt–glucose solution and salt–water solution was different, calibrating the conductivity in a certain concentration of glucose solution would ensure the accuracy of the experiments. We measured the conductivity of a series of solutions of glucose with predetermined amount of salts. It was found that the amount of salt added and the conductivity showed a nearly linear relationship to the salt concentration. This allowed us to determine the salt rejection in our FO process via interpolation.

Duplicated tests were carried out in this experiment and average results are reported with standard deviation lower than 10%.

2.4. Scanning electron microscopy

CTA membranes tend to deform and become brittle upon drying at room temperature. To minimize the morphological change, the freeze-drying technique was utilized. Membrane pieces were fractured in liquid nitrogen and stored in a round bottom flask. The flask with the membrane was connected to the

vacuum system in the freeze dryer and the flask was immediately kept in liquid nitrogen to maintain a low temperature. After 12 h, the flask was disconnected and the samples were then coated with a thin gold layer for SEM imaging. For images of low magnifications, Hitachi TM1000 Scanning Electron Microscopy (SEM) was used. High-resolution images were recorded using a Field Emission Scanning Electron Microscopy (FESEM, Hitachi S-4800).

3. Results and discussion

3.1. Effect of CTA/CA ratio

Cellulose acetate (CA) and cellulose triacetate (CTA) are very close in chemical structure yet CA is more hydrophilic than CTA. Their main difference CTA has a higher degree of acelation than CA. For FO membrane preparation, we initially tried to make a blend membrane by varying the weight ratio of CTA/CA but fixing the total polymer content at 13.8 wt.%: CTA/CA 1/1, 3/1, 7/1, and 1/0. Other components in the membrane solution were dioxane 55.5 wt.%, acetone 19.1 wt.%, lactic acid 3 wt.%, and methanol 8 wt.%. The FO performance of obtained membranes was characterized using 2 M glucose as the draw solution and 0.5 M NaCl aqueous solution as feed on the active layer of membrane (AL-FS mode) at 50 °C unless stated otherwise. As shown in Fig. 2, with the increase of CA content, the membrane water permeation increased from about 7 to 14 kg/m^2 h, but the salt rejection dropped from 97% to nearly zero (Fig. 2).

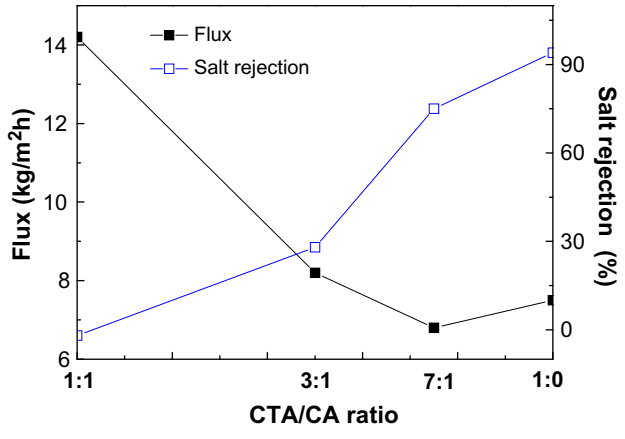

Fig. 2. CTA/CA membrane FO fluxes and NaCl rejection as a result of CTA/CA ratio. AL-FS mode; casting composition: dioxane/acetone: 2.9/1; lactic acid: 3 wt.%; methanol: 8.6 wt.%; evaporation time: 0 s; water bath temperature: 12 °C.

CA is more hydrophilic than cellulose triacetate because of the presence of hydroxyl groups. Literature work has shown that acylation degree is directly related to the salt rejection rate and water flux of the membrane in that higher acylation degree lead to higher salt rejection rate [26,27]. In comparison, our results showed similar trend that the addition of CA helps to improve the membrane permeability however with the sacrifice of the salt rejection. Similarly, the double-skinned CA membranes reported by Wang et al. [24] have shown the same problem as a high water flux accompanied by a high reverse solute diffusion (salt leakage). We believe that the presence of hydroxyl groups might be the reason for the salt leakage in the FO process, however, membrane structure and morphological difference may play roles as well.

The acylation degree of CTA is 43.3% and for CA is 39.2%. Such a slight variation may lead to the significant change in the phase separation behavior during immersion precipitation, both thermodynamically and kinetically. The resulted membrane morphology and structure is most probably different: for example, a slightly more hydrophilic CA membrane may lead to a more swollen and loose skin layer, thus the membrane permeability is high but at a low rejection rate. Detailed research on this issue will be published soon. Our membranes based on solely CTA materials showed high NaCl rejection and acceptable water flux. Thus, in the following paragraph, CTA, instead of CTA/CA blend, will be used as the polymer for FO membrane preparation.

It should be noted that the operation mode in our case is AL-FS mode. It is known that for FO processes, due to severer ICP in the AL-FS mode, it normally shows much lower flux and rejection than AL-DS mode [17]. Since it is our objective to find a suitable FO membrane with less ICP, we have adopted the AL-FS mode for further optimization of the performance of the membrane.

3.2. Effect of CTA concentration

In this part, the effects of CTA content were investigated on flux and salt rejection. Fig. 3 shows CTA concentration between 11.8 and 15.8 wt.%. Fig. 3 shows the effect of CTA concentration on the FO performance. Surprisingly, neither the water flux nor the salt rejection varied much with respect to the viscosity change. Solution viscosity was measured and nearly 10 times increase in the solution viscosity was observed when the CTA concentration increased only 4 wt.%. However, since the CTA membrane has relatively dense skin layers which controls the permeation

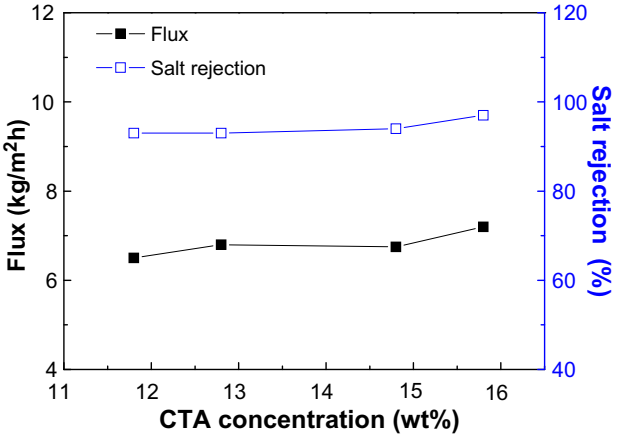

Fig. 3. CTA membrane FO fluxes and NaCl rejection as a result of CTA concentration. AL-FS mode; casting solution composition: dioxane/acetone: 2.9/1, lactic acid: 3 wt.%, methanol: 8.6 wt.%, evaporation time: 0 s, water bath temperature: 12˚C.

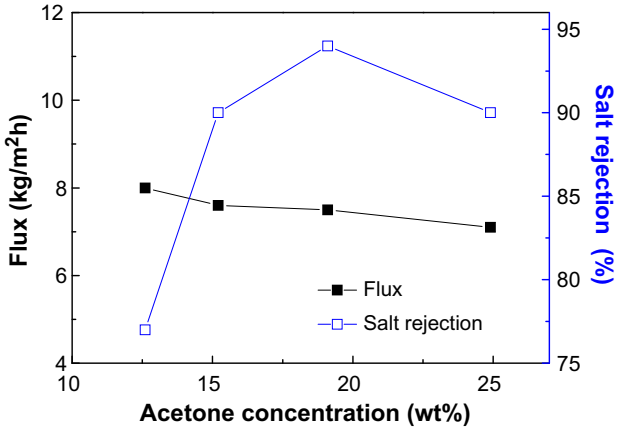

Fig. 4. CTA membrane FO fluxes and NaCl rejection as a result of different acetone concentration. AL-FS mode; cast solution composition: CTA: 13.8 wt.%; dioxane and acetone: 74.6 wt.%, lactic acid: 3 wt.%; methanol: 8.6 wt.%, evaporation time: 0 s, water bath temperature: 12˚C.

and separation characteristics of the membranes, the 11.8 wt.% CTA in the polymer solution is probably enough to form a dense skin layer. Moreover, CTA is relatively hydrophilic. The phase inversion process of CTA solution may be different from hydrophobic polymers in water, thus the viscosity difference might play less significant role. Therefore, a high viscosity does not necessarily correspond to a dense membrane skin layer, or low water permeability. In further investigations, the CTA content was fixed at 13.8 wt.% with the solution viscosity of around 30,000 cp.

3.3. Effect of acetone

By maintaining the total dioxane and acetone percentage at 74.6 wt.% and varying their ratio, the effect of the acetone concentration on the membrane performance was investigated. Methanol and lactic acid were 8 and 3 wt.%, respectively. As shown in Fig. 4, with the increase of the acetone content from 13 to 25 wt.%, a slight decrease in water flux was observed (from 8 to 7 $kg/m^2 h$). The rejection rate changed significantly. At low acetone content, the rejection rate increased with acetone concentration, and a maximum was observed at approximately 19.1 wt.%. Thereafter, the rejection rate declined.

In general, the membrane flux and rejection are in a trade-off relationship: high flux correlates to low rejection rate. In this case, it can also be seen that with the decrease of water flux, higher salt rejection rates are observed as well. However, the effects in salt rejection rate are more pronounced. The membrane flux/salt rejection is related to the membrane mass transfer resistance and eventually the subtle membrane structure. How acetone/dioxane ratio affects the membrane structure is not clearly understood. Since acetone is highly volatile, the time after casting and before immersion precipitation is critical for controlling the membrane performance as discussed below.

3.4. Evaporation time

Acetone is highly volatile and its evaporation rate is influenced by both environment humidity and temperature. The ambient conditions at 25˚C and a relative humidity of 60% were maintained throughout

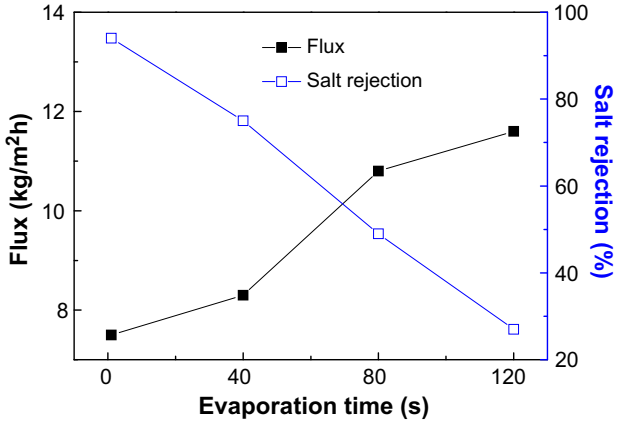

Fig. 5. CTA membrane FO fluxes and NaCl rejection as a result of evaporation time. AL-FS mode; cast solution composition: CTA: 13.8 wt.%, dioxane: 55.5 wt.%, acetone: 19.1 wt.%, lactic acid: 3 wt.%, methanol: 8.6 wt.%, water bath temperature: 12˚C.

this investigation. Fig. 5 shows the effect of the evaporation time on membrane performance. With an increase in evaporation time, the membrane flux rapidly increased and rejection rate drastically declined. Reports have shown that the evaporation of acetone has two contradictory effects on membrane characteristics [28]: (1) evaporation of acetone increases the number of aggregation pores in the membrane surface and (2) excessive evaporation results in pores reunion, hence the numbers of pores decreases and the pore size increases. As seen in Fig. 5, the membrane flux increases almost linearly with the increase of evaporation time. The results indicate that 40 s of evaporation might have caused aggregation pore reunion and thereby low salt rejection.

3.5. Effect of lactic acid and methanol concentration

Fig. 6 shows the effect of lactic acid concentration on membrane properties. With the increase of lactic acid content, the membrane flux increased rapidly. The membrane rejection showed a different scenario: at lactic acid concentration lower than 3 wt.%, the rejection were in the range between 95% and 98%; with further increase in the lactic acid concentration, the rejection declined. Kastelan-Kunst et al. [29,30] found that the lactic acid acts both as a proton donor and a proton acceptor because of the its carbonyl and hydroxyl groups. It can thus form chain-like structure with adjacent CTA molecules and a loose superamolecular network in the solution which leads to a selective layer of high porosity, high flux, and low rejection rate. With the increase of lactic acid concentration, both the size and number of pores increase, and thus higher flux and lower rejection rate are observed.

Fig. 7 shows the effect of methanol concentration on membrane properties. Without methanol addition, the flux was about 1.4 $kg/m^2 h$, at 10 wt.%, the water flux was about 7 $kg/m^2 h$. With the increase of methanol concentration, the membrane flux appeared to increase almost linearly. Similar to lactic acid, the rejection rates initially increased slightly and then declined with the further increase of methanol. However, the salt rejection of the CTA membrane stayed above 95%. The role of methanol and lactic acid are similar: both are nonsolvents and pore-forming agents. When the methanol concentration exceeded 10 wt.%, in the casting solution, insoluble transparent particles or gels were observed. This observation agrees with Duarte et al. [27] and Vásárhelyi et al.'s findings [31].

Table 1 lists the dispersive (δ_d), dipole–dipole (δ_p), hydrogen bonding (δ_h), and total (δ_{sp}) solubility parameters for each chemicals and materials used in the final polymer solution for the preparation of a FO membrane. The δ_{sp} of cellulose triacetate is 18.8 $(MPa)^{1/2}$, which is very similar to the total solubility parameter for dioxane (20.5 $MPa^{1/2}$) and acetone (20.1 $MPa^{1/2}$). The solubility parameters of methanol (29.7 $MPa^{1/2}$) and lactic acid (34.1 $MPa^{1/2}$) are significantly higher than that of CTA, thus behaves as the nonsolvent for the polymer. The Hansen solubility parameter values listed in Table 1 indicate that acetone and dioxane are good solvent to CTA due to the close dispersive interaction between the solvent and polymer. However, the large difference in hydrogen bonding between CTA and methanol and lactic acid

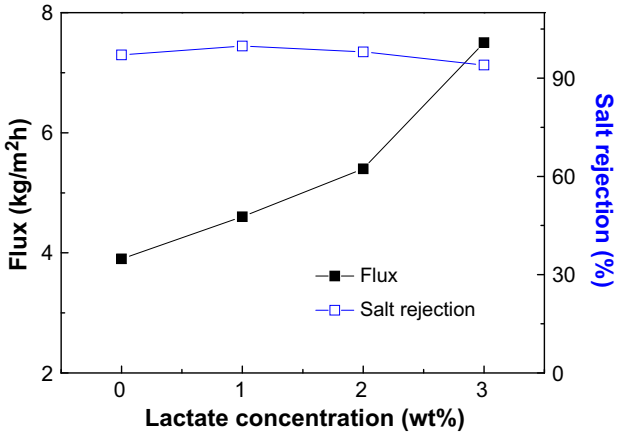

Fig. 6. CTA membrane FO fluxes and NaCl rejection as a result of lactic acid concentration. AL-FS mode; cast solution composition: CTA: 13.8 wt.%, dioxane/acetone: 2.9/1, methanol: 8.6 wt.%, evaporation time: 0 s, water bath temperature: 12˚C.

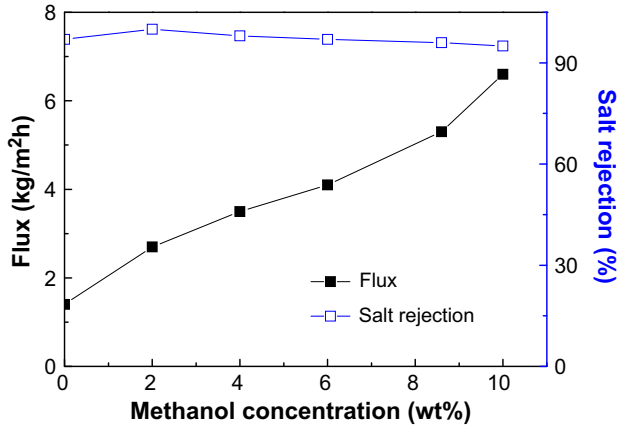

Fig. 7. CTA membrane FO fluxes and NaCl rejection as a result of methanol concentration. AL-FS mode; cast solution composition: CTA: 13.8 wt.%, dioxane/acetone: 2.9/1, lactic acid: 2 wt.%, evaporation time: 0 s, water bath temperature: 12˚C.

Table 1
Hansen solubility parameters of chemicals and materials using the polymer solution [34,35]

Chemicals and materials	δ_d (MPa$^{1/2}$)	δ_p (MPa$^{1/2}$)	δ_h (MPa$^{1/2}$)	δ_{sp} (MPa$^{1/2}$)
Cellulose triacetate	15.6	–	10.6	18.8
Dioxane	19.0	1.8	7.4	20.5
Acetone	15.5	10.4	7.0	20.1
Lactic acid	17.0	8.3	28.4	34.1
Methanol	15.1	12.3	22.3	29.7
Mixture solvent	–	–	–	18.8

Note: δ_d: dispersive parameter; δ_p: polar parameter; δ_h: hydrogen bonding parameter; δ_{sp}: total solubility parameter.
Mixture solvent is the solvent used for preparation of the polymer solution. The compostion of the polymer solution was: CTA: 13.8 wt.%, dioxane: 59.4 wt.%, acetone: 15.2 wt.%, lactic acid: 3 wt.%, methanol: 8.6 wt.%. The calculation of the total solubility parameter is based on summation of the concentration ratio multiplying with the solubility parameter of each chemical.

may explain that the two are nonsolvents to CTA. Based on the contribution of the concentration ratio, the summation of the total solubility parameters of the mixture solvent was 18.8 MPa$^{1/2}$, which is the same as that of CTA. During the experiment, it has been noticed that slightly higher concentration of the methanol or lactic acid would lead to an instantaneous gelation of the polymer solution. Therefore, the content of methanol and lactic acid must be carefully controlled during the solution preparation. With this composition, the effect of the coagulation bath temperature on the membrane performance is investigated.

3.6. Coagulation bath temperature

Water is used as the coagulant and the coagulation bath temperature effects were studied on the CTA membrane FO flux and salt rejection (Fig. 8). With the increase in water bath temperature from 1 to 20°C, the membrane flux rapidly decreased from 9.5 to 6.0 kg/m^2 h. The rejection rate increased from 70% to 90% and stayed unchanged in the range of 12°C and 20°C. In general, the flux and rejection change correlates each other well in that a higher flux corresponds to a lower salt rejection. It is well known that the coagulation bath temperature is a key parameter in determining the membrane properties which affects the phase inversion thermodynamics and eventually the membrane structure. The bath temperature affects not only the exchange rate of the solvent–nonsolvent, but also the motion of the polymer chains. Thermodynamically, a higher temperature favors the quick motion of the polymer chains which enables the rearrangement of the polymer chain at the skin layer before the CTA chains are completely fixed by gelation or glassification. However, it has been shown detrimental effects: high temperature has resulted in lower water permeability [32].

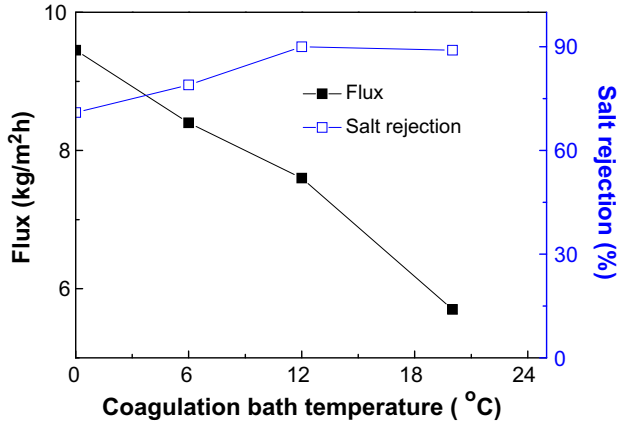

Fig. 8. CTA membrane FO fluxes and NaCl rejection as a result of water bath temperature. AL-FS mode; cast solution composition: CTA: 13.8 wt.%, dioxane: 59.4 wt.%, acetone: 15.2 wt.%, lactic acid: 3 wt.%, methanol: 8.6 wt.%; evaporation time: 0 s.

Fig. 9(a–d) shows the SEM photos of the cross-section of the CTA membranes prepared at various coagulation bath temperatures. It can be seen that the CTA membrane has a typical three-layered sandwich structure: two relatively dense skin layers and a mid-layer with macrovoids. It was interesting to observe that the size of the voids increase with the water bath temperature. No clear changes in dense selective layer were found. The top and bottom surfaces are quite dense. At a magnification of 30 k, uneven surface with nodules is observed at both top and bottom surfaces (Fig. 9(e and f)). No clear pores are visible in both surfaces, but the bottom surfaces appeared to be rougher than the top surface. The cause of this difference is not yet clear, however, may be related to the difference between the water phase and the glass casting plate.

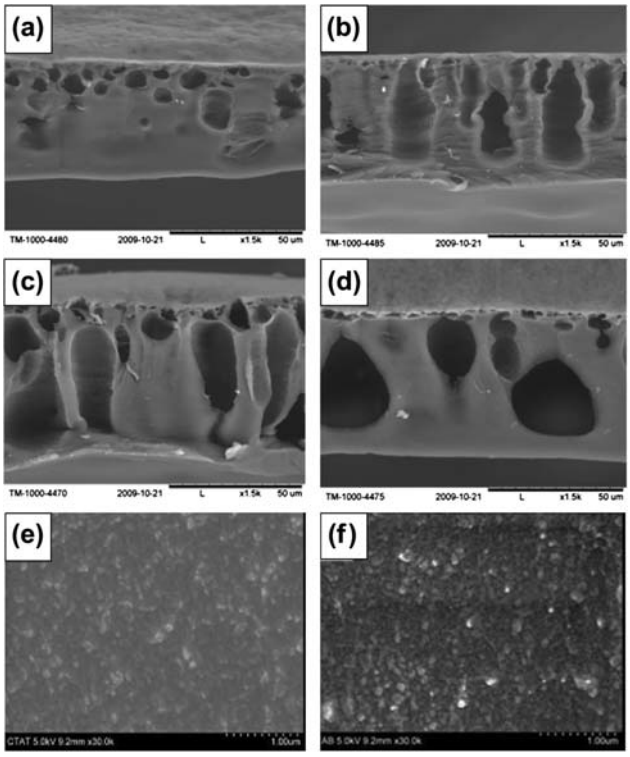

Fig. 9. SEM images of CTA membrane. (a-d) cross-section view at different water bath temperature. (a) 1℃, (b) 6℃, (c) 12℃, (d) 20℃. (e and f) Top surface and bottom surface of (b) at 30 k magnification, respectively.

Overall, to prepare a high flux CTA membrane with relatively high rejection, a water bath at a low temperature is preferred.

3.7. FO performance of CTA membrane

The properties of the CTA membrane with sandwiched structure were characterized in comparison with the commercial HTI flat-sheet membrane. An aqueous 0.5 M NaCl solution was used as the feed and a 2 M glucose solution was used as the draw solution. In FO tests, both AL-DS mode and AL-FS mode were carried out [33]: as can be seen in Fig. 10, the CTA membranes showed twice as high water flux (15.2 $kg/m^2 h$) as the HTI membrane (7.5 $kg/m^2 h$) in the AL-DS mode and a slightly higher rejection rate for NaCl. In the AL-DS mode, NaCl solution is in direct contact with membrane porous support layer (or the layer opposite to the skin layer). In the AL-DS mode, concentrative internal concentration polarization occurred, thus a concentration gradient of NaCl inside the pores and the bulk feed solution is built up. Eventually, the loss of effective osmotic pressure and low draw efficiency are resulting in. In AL-FS mode, the CTA membrane showed a flux of 7.6 $kg/m^2 h$, which was nearly 50% of that at AL-DS mode, and the HTI membrane showed a flux of 3.35 $kg/m^2 h$, only 40% as that in AL-DS mode. This result indicates that the CTA membrane has a slightly lower degree of ICP than HTI membrane, which may be due to the denser bottom surface than HTI membranes. In AL-FS mode, the glucose solution was in direct contact with the CTA membrane bottom surface, dilutive ICP is expected leading to lower effective osmotic pressure than AL-DS mode [17].

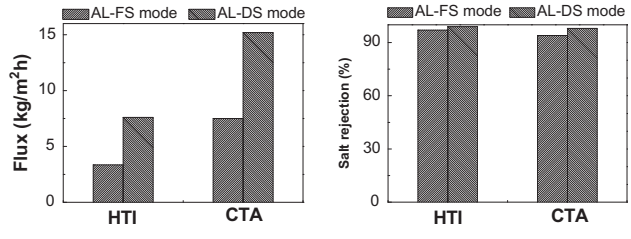

Fig. 10. Comparison of water fluxes and NaCl rejections of the HTI's FO membrane and our CTA membrane. ▨0.5 M NaCl on active layer (AL-FS mode); ▧0.5 M NaCl on support layer (AL-DS mode).

The higher than HTI membrane flux may be understood by the different membrane morphology. Ideally, the two perfectly dense skin layers in the CTA membrane can effectively avoid ICP with improved draw efficiency. The macrovoids allow quick diffusion of the water, thus high water permeability. In reality, although a double-skinned structure is observed for the CTA membrane, it appeared that the diffusion of salt and/or glucose into the substructure still took place given the lower than 100% salt rejection. Taking this CTA membrane as a model, we are currently working on novel draw solutes with bulky structure in order to improve the FO efficiency. By avoiding the penetration of the draw solute into the porous structure, much higher flux may be achieved.

4. Conclusions

In this paper, a systematic investigation was carried out on the preparation of cellulose triacetate membranes. Parameters were investigated including polymer blend ratio, concentrations of the solvents, nonsolvents, and the polymer content in the dope solution with respect to the membrane performance in FO process. It was found that addition of cellulose acetate improved membrane flux but led to low rejection. CTA concentration in the polymer solution had little impact on membrane flux and rejection rate within the range of investigation. At an appropriate concentration, lactic acid and methanol could

significantly improve FO fluxes without much loss in the rejection rate. Furthermore, extended evaporation time reduced rejection rate due to loss of acetone and relatively lower water bath temperature led to high water permeability but low rejection.

The CTA membrane showed higher flux than commercial HTI membranes. Morphological study indicates that the CTA membrane showed a three layer structure consisting of two dense skin layers and a very open mid-layer, which may explain its high FO flux. Further improvement in membrane performance will be focused on the preparation of ideal double-skinned membrane and evaluate its performance in combination with bulky draw solutes.

Acknowledgments

This research is partially supported by Natural Science Foundation China (Project Nos. 20976083, 21176119), National Key Basic Research Program of China 973 (Nos. 2012CB932800, 2009CB623402), China–Israel Joint Research Funds Supported by Ministry of Science and Technology China (Project No.: 2010-01).

References

[1] R.E. Kravath, J.A. Davis, Desalination of sea water by direct osmosis, Desalination 16 (1975) 151–155.
[2] G.D. Mehta, S. Loeb, Performance of Permasep B-9 and B-10 membranes in various osmotic regions and at high osmotic pressures, J. Membr. Sci. 4 (1979) 335.
[3] G.D. Mehta, Further results on the performance of present-day osmotic membranes in various osmotic regions, J. Membr. Sci. 10 (1982) 3–19.
[4] J.-J. Qin, W.C.L. Lay, K.A. Kekre, Recent developments and future challenges of forward osmosis for desalination: A review, Desalin. Water Treat. 39 (2012) 123–136.
[5] E.R. Cornelissen, D. Harmsen, K.F. de Korte, C.J. Ruiken, J.-J. Qin, H. Oo, L.P. Wessels, Membrane fouling and process performance of forward osmosis membranes on activated sludge, J. Membr. Sci. 319 (2008) 158–168.
[6] C.R. Martinetti, A.E. Childress, T.Y. Cath, High recovery of concentrated RO brines using forward osmosis and membrane distillation, J. Membr. Sci. 331 (2009) 31–39.
[7] A. Achilli, T.Y. Cath, E.A. Marchand, A.E. Childress, The forward osmosis membrane bioreactor: A low fouling alternative to MBR processes, Desalination 239 (2009) 10–21.
[8] J.J. Qin, K.A. Kekre, M.H. Oo, G. Tao, C.L. Lay, C.H. Lew, E.R. Cornelissen, C.J. Ruiken, Preliminary study of osmotic membrane bioreactor: Effects of draw solution on water flux and air scouring on fouling, Water Sci. Technol. 62 (2010) 1353–1360.
[9] D. Xiao, C.Y. Tang, J. Zhang, W.C.L. Lay, R. Wang, A.G. Fane, Modeling salt accumulation in osmotic membrane bioreactors: Implications for FO membrane selection and system operation, J. Membr. Sci. 366 (2011) 314–324.
[10] K.B. Petrotos, P. Quantick, H. Petropakis, A study of the direct osmotic concentration of tomato juice in tubular membrane – module configuration. I. The effect of certain basic process parameters on the process performance, J. Membr. Sci. 150 (1998) 99–110.
[11] K.B. Petrotos, A.V. Tsiadi, E. Poirazis, D. Papadopoulos, H. Petropakis, P. Gkoutsidis, A description of a flat geometry direct osmotic concentrator to concentrate tomato juice at ambient temperature and low pressure, J. Food Eng. 97 (2010) 235–242.
[12] T.Y. Cath, A.E. Childress, M. Elimelech, Forward osmosis: Principles, applications, and recent developments, J. Membr. Sci. 281 (2006) 70–87.
[13] D.A. LaVan, T. McGuire, R. Langer, Small-scale systems for in vivo drug delivery, Nat. Biotechnol. 21 (2003) 1184–1191.
[14] N.Y. Yip, A. Tiraferri, W.A. Phillip, J.D. Schiffman, L.A. Hoover, Y.C. Kim, M. Elimelech, Thin-film composite pressure retarded osmosis membranes for sustainable power generation from salinity gradients, Environ. Sci. Technol. 45 (2011) 4360–4369.
[15] J.R. McCutcheon, R.L. McGinnis, M. Elimelech, Desalination by ammonia–carbon dioxide forward osmosis: Influence of draw and feed solution concentrations on process performance, J. Membr. Sci. 278 (2006) 114–123.
[16] J.R. McCutcheon, M. Elimelech, Modeling water flux in forward osmosis: Implications for improved membrane design, AlChE J. 53 (2007) 1736–1744.
[17] G.T. Gray, J.R. McCutcheon, M. Elimelech, Internal concentration polarization in forward osmosis: Role of membrane orientation, Desalination 197 (2006) 1–8.
[18] K. Gerstandt, K.V. Peinemann, S.E. Skilhagen, T. Thorsen, T. Holt, Membrane processes in energy supply for an osmotic power plant, Desalination 224 (2008) 64–70.
[19] S. Zhang, K.Y. Wang, T.-S. Chung, H. Chen, Y.C. Jean, G. Amy, Well-constructed cellulose acetate membranes for forward osmosis: Minimized internal concentration polarization with an ultra-thin selective layer, J. Membr. Sci. 360 (2010) 522–535.
[20] N.Y. Yip, A. Tiraferri, W.A. Phillip, J.D. Schiffman, M. Elimelech, High performance thin-film composite forward osmosis membrane, Environ. Sci. Technol. 44 (2010) 3812–3818.
[21] R. Wang, L. Shi, C.Y. Tang, S. Chou, C. Qiu, A.G. Fane, Characterization of novel forward osmosis hollow fiber membranes, J. Membr. Sci. 355 (2010) 158–167.
[22] C. Qiu, S. Qi, C.Y. Tang, Synthesis of high flux forward osmosis membranes by chemically crosslinked layer-by-layer polyelectrolytes, J. Membr. Sci. 381 (2011) 74–80.
[23] C.Y. Tang, Q. She, W.C.L. Lay, R. Wang, R. Field, A.G. Fane, Modeling double-skinned FO membranes, Desalination 283 (2011) 178–186.
[24] K.Y. Wang, R.C. Ong, T.-S. Chung, Double-skinned forward osmosis membranes for reducing internal concentration polarization within the porous sublayer, Ind. Eng. Chem. Res. 49 (2010) 4824–4831.
[25] J. Su, T.-S. Chung, B.J. Helmer, J.S. de Wit, Enhanced double-skinned FO membranes with inner dense layer for wastewater treatment and macromolecule recycle using sucrose as draw solute, J. Membr. Sci. 396 (2012) 92–100.
[26] H.K. Lonsdale, H.E. Podall, Reverse Osmosis Membrane Research, Plenum Press, New York, 1972.
[27] A.P. Duarte, M.T. Cidade, J.C. Bordado, Cellulose acetate reverse osmosis membranes: Optimization of the composition, J. Appl. Polym. Sci. 100 (2006) 4052–4058.
[28] T.A. Tweddle, W.S. Peterson, A.E. Fouda, S. Sourirajan, Effect of casting variables on the performance of tubular cellulose acetate reverse osmosis membranes, Ind. Eng. Chem. Prod. Res. Develop. 20 (1981) 496–501.
[29] L. Kastelan-Kunst, D. Sambrailo, B. Kunst, On the skinned cellulose triacetate membranes formation, Desalination 83 (1991) 331–342.

[30] L. Kastelan-Kunst, V. Dananic, B. Kunst, K. Kosutic, Preparation and porosity of cellulose triacetate reverse osmosis membranes, J. Membr. Sci. 109 (1996) 223–230.
[31] K. Vásárhelyi, J.A. Ronner, M.H.V. Mulder, C.A. Smolders, Development of wet–dry reversible reverse osmosis membrane with high performance from cellulose acetate and cellulose triacetate blend, Desalination 61 (1987) 211–235.
[32] J. Su, Q. Yang, J.F. Teo, T.-S. Chung, Cellulose acetate nanofiltration hollow fiber membranes for forward osmosis processes, J. Membr. Sci. 355 (2010) 36–44.
[33] J.R. McCutcheon, M. Elimelech, Influence of concentrative and dilutive internal concentration polarization on flux behavior in forward osmosis, J. Membr. Sci. 284 (2006) 237–247.
[34] J. Brandrup, E.H. Immergut, E.A. Grulke, A. Abe, D.R. Bloch, Polymer Handbook, fourth ed., John Wiley & Sons, 2005.
[35] C.M. Hansen, Hansen Solubility Parameters: A User's Handbook, second ed., CRC Press, Taylor & Francis Group, 2007.